ISSN: 1410-8917
e-ISSN: 2597-9914

Jurnal Kimia Sains dan Aplikasi 28 (5) (2025): 274-282

Jurnal Kimia Sains dan Aplikasi
Journal of Scientific and Applied Chemistry

Journal homepage: http://ejournal.undip.ac.id/index.php/ksa

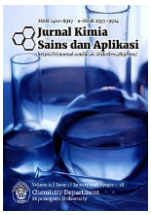

Synthesis of NaX Zeolite from Blitar Kaolin via Hydrothermal and Sonication Methods with Alkali Fusion Pre-treatment

Susi Nurul Khalifah [1,*], Saidun Fiddaroini [2], Aminatus Arifah [1], Awwali Maf'ulah Hasanah [1], Anton Prasetyo [1]

[1] Chemistry Study Program, Faculty of Science and Technology, Maulana Malik Ibrahim State Islamic University, Malang (65144), Indonesia
[2] Department of Chemistry, Faculty of Mathematics and Natural Sciences, Brawijaya University, Malang (65145), Indonesia

* Corresponding author: susikhalifah@kim.uin-malang.ac.id

https://doi.org/10.14710/jksa.28.5.274-282

Article Info

Article history:

Received: 18th January 2025
Revised: 25th June 2025
Accepted: 30th June 2025
Online: 10th July 2025

Keywords:
Zeolite NaX; Kaolin, Hydrothermal; Sonication; Alkali Fusion

Abstract

NaX zeolite, widely recognized for its applications in cation exchange, adsorption, and catalysis, was successfully synthesized from Blitar natural kaolin using an alkali fusion pre-treatment, followed by two comparative synthesis methods: hydrothermal and sonication. The synthesis was conducted at 70°C for 2 and 4 hours. Optimal conditions were achieved with a NaOH/kaolin weight ratio of 2.0 and a synthesis gel composition of $10SiO_2$: $1Al_2O_3$: $6Na_2O$: $180H_2O$ (molar ratio). X-ray diffraction (XRD) confirmed the transformation of natural kaolin into sodium silicate, with sonication yielding phase-pure NaX zeolite, while the hydrothermal method resulted in NaX with sodalite impurities. Fourier-transform infrared (FTIR) spectroscopy identified characteristic NaX vibrations, and scanning electron microscopy (SEM) revealed cubic-shaped particles in the sonication method. The sonication process accelerated crystallization, producing higher-purity zeolite in shorter times than hydrothermal synthesis. These findings emphasize the effectiveness of sonication in enhancing the crystallinity and purity of NaX zeolite, offering a robust, time-efficient alternative for large-scale zeolite production.

1. Introduction

Zeolites are porous aluminosilicate minerals composed of interconnected alumina and silica tetrahedra sharing oxygen atoms [1, 2]. Among various zeolite types, NaX zeolite stands out for its significant applications. The synthesis of NaX zeolite has garnered considerable attention due to its unique properties, including high catalytic activity [3], large surface area [4], elevated surface energy [5], and acidic characteristics [6]. These properties make NaX zeolite widely used in applications such as cation exchange [7], adsorption [8], molecular sieving [9], and as a catalyst in gas separation and organic compound processing [10].

NaX zeolite is traditionally synthesized using high-cost chemical precursors such as colloidal silica, sodium silicate, and tetraethyl orthosilicate (TEOS) as silica sources, along with aluminate, gamma alumina, alumina trihydrate, and sodium aluminate for the alumina component [4, 11]. These chemical sources, while effective, contribute significantly to the overall cost of the synthesis process. To address this, more economical raw materials such as natural clay minerals have been explored [12], with Blitar kaolin emerging as a promising alternative [13].

Blitar kaolin, sourced from East Java, Indonesia, is abundant and relatively inexpensive, making it a promising alternative to conventional silica-alumina sources for zeolite production. The high Si/Al ratio of approximately 3.25 further supports its suitability for NaX zeolite synthesis. In addition to its chemical appropriateness, the wide availability of kaolin in Indonesia ensures a steady and sustainable raw material supply, potentially reducing production costs and promoting localized, eco-friendly industrial applications.

However, the primary challenge in synthesizing zeolite from kaolin lies in the high quartz content [14],

which acts as an impurity and can adversely affect the purity and quality of the final product [15]. To mitigate this, an alkali fusion pre-treatment is employed, where NaOH is mixed with the kaolin, followed by a calcination step [16, 17]. This process helps to convert the kaolin into a more reactive form by removing or reducing its quartz content [18].

Previous studies have used NaOH/kaolin ratios of 1.7 and 1.2, which, although effective in synthesizing zeolite, still resulted in the presence of quartz impurities [16]. The alkali fusion pre-treatment is essential for transforming inert kaolin, especially its quartz component, into a reactive amorphous sodium silicate phase by thermal activation with sodium hydroxide. This process improves the availability of silicon and aluminum species for zeolite framework formation and has been shown to enhance crystallinity and phase purity in subsequent synthesis steps [18].

The crystallization process in zeolite synthesis can be optimized using different methods, primarily hydrothermal [19] and sonication techniques [20]. The hydrothermal method, widely used and well-documented, involves the use of high temperature and pressure in a hydrothermal reactor to promote the formation of zeolite crystals [21]. In contrast, the sonication method employs ultrasound energy to accelerate the reaction between the chemical components, enhancing the crystallization process at a faster rate [22]. While the hydrothermal method has been extensively reported in the literature for NaX zeolite synthesis, the use of sonication remains relatively less explored [23, 24]. By comparing these methods under controlled conditions, this work aims to determine optimal strategies for producing high-purity, crystalline NaX zeolite.

This study aims to synthesize high-purity NaX zeolite from Blitar kaolin by employing two synthesis routes—hydrothermal and sonication—following alkali fusion pre-treatment. The alkali fusion step enhances the reactivity of kaolin by converting it into sodium silicate, while the subsequent crystallization methods are evaluated in terms of their efficiency, phase purity, and morphology. By analyzing the effects of crystallization time, this work provides a comparative assessment and determines the optimal conditions for efficient, scalable NaX zeolite synthesis.

These parameters were evaluated using X-ray diffraction (XRD), Fourier-transform infrared (FTIR) spectroscopy, and scanning electron microscopy (SEM) to comprehensively analyze the structural and morphological characteristics of the synthesized materials. This study aims to provide a comparative analysis of both methods and determine the optimal conditions for obtaining high-purity NaX zeolite. To systematically investigate the influence of alkali concentration, this study varied the NaOH/kaolin weight ratio (1.0, 2.0, and 3.0) during the fusion process, which significantly impacted quartz removal and precursor reactivity.

2. Experimental

2.1. Materials and Instrumentations

Kaolin, sourced from Blitar, East Java, Indonesia, was ground to a particle size of 200–300 mesh to serve as the starting material. Sodium hydroxide (NaOH; Merck, >99%), aluminum oxide (Al_2O_3; Merck, 99%), and distilled water were also used in the synthesis process. The identification of the zeolite phase was conducted via X-ray diffraction (XRD) using a Philips diffractometer equipped with Cu-Kα radiation (Philips XRG 3100) over a 2θ range of 5° to 60°. Infrared (IR) spectra were obtained using a Perkin Elmer Spectrum GX Fourier-transform infrared (FTIR) spectrometer. The morphology of both kaolin and the synthesized products was examined using a Hitachi S-570 scanning electron microscope (SEM) operated at 15 kV.

2.2. Alkali Fusion Process

To investigate the impact of alkali concentration on the reactivity of kaolin, samples were prepared with NaOH/kaolin weight ratios of 1.0, 2.0, and 3.0, as summarized in Table 1. The NaOH and kaolin were thoroughly mixed and ground for 30 minutes to ensure homogeneity before thermal treatment. The mixtures were then subjected to alkali fusion at 600°C for 1 hour, a process designed to disrupt the crystalline structure of kaolin and facilitate the formation of sodium silicate (Na_2SiO_3).

Post-fusion, the resultant products were re-grounded to achieve a uniform particle size and subsequently characterized using a comprehensive suite of analytical techniques. XRD was employed to identify phase transformations and quantify the reduction of quartz impurities. FTIR provided insights into the chemical bond alterations and the emergence of sodium silicate-specific vibrations. SEM was utilized to examine the morphological changes induced by the alkali fusion process. This systematic approach to sample preparation and characterization ensures a detailed understanding of the structural and compositional evolution of kaolin under varying alkali conditions, laying the groundwork for optimizing precursor materials in zeolite synthesis.

2.3. Reaction Pathways for NaX Zeolite Formation

During the alkali fusion pre-treatment stage, kaolin ($Al_2Si_2O_5(OH)_4$) is mixed with NaOH and heated at high temperatures. This process facilitates the breakdown of the kaolin structure and the removal of quartz impurities. The reaction produces Na_2SiO_3 and aluminum hydroxide ($Al(OH)_3$), which are more reactive precursors for zeolite synthesis. The reaction (1) is represented in Equation (1).

Table 1. Weight of NaOH and kaolin

Weight ratio of NaOH/Kaolin	Weight of NaOH (g)	Weight of kaolin (g)
1.0	4.29	4.29
2.0	8.58	4.29
3.0	12.87	4.29

$$Al_2Si_2O_5(OH)_4 + 4NaOH \rightarrow 2Na_2SiO_3 + 2Al(OH)_3 \quad (1)$$

This transformation improves the reactivity of the kaolin by converting it into an amorphous phase, mainly Na_2SiO_3, which is essential for the crystallization of zeolite frameworks.

Following alkali fusion, the resulting Na_2SiO_3 is used as a precursor for NaX zeolite synthesis. In this stage, Na_2SiO_3 reacts with Al_2O_3, NaOH, and water. Using a molar ratio of $10SiO_2$: $1Al_2O_3$: $6Na_2O$: $180H_2O$, the components are aged and then subjected to two different crystallization methods: hydrothermal and sonication. The overall reaction is described by the chemical equation shown in Equation (2).

$$Na_2SiO_3 + Al_2O_3 + NaOH + H_2O \rightarrow NaX\ Zeolite \quad (2)$$

In the hydrothermal method, this reaction occurs under moderate heating (70°C) in a sealed environment, allowing crystal growth over time. In contrast, the sonication method uses ultrasonic irradiation (42 kHz, 100 W) to accelerate the reaction, enhancing nucleation and reducing synthesis time while achieving comparable or superior crystallinity.

2.4. Synthesis of NaX Zeolite

The alkali fusion product prepared with a NaOH/kaolin weight ratio of 2.0 was selected as the precursor for NaX zeolite synthesis. The synthesis was conducted using a molar composition of $10SiO_2$: $1Al_2O_3$: $6Na_2O$: $180H_2O$, which is optimized for the formation of NaX zeolite. The precursor mixture was aged at ambient temperature (~30°C) for 10 days to allow uniform gelation and enhanced nucleation.

The hydrothermal method involves crystallization under controlled thermal conditions in a sealed reactor. The precursor gel, prepared from the alkali fusion product, Al_2O_3, NaOH, and water in a molar ratio of $10SiO_2$: $1Al_2O_3$: $6Na_2O$: $180H_2O$, was transferred into a hydrothermal reactor. The system was heated at 70°C for 2 and 4 hours, respectively. This method allows slow and uniform crystal growth under moderate pressure and is commonly used in conventional zeolite synthesis.

The sonication method uses ultrasonic waves to accelerate the nucleation and crystallization of NaX zeolite. Using the same precursor composition as in the hydrothermal method, the mixture was exposed to ultrasonic irradiation at a frequency of 42 kHz and power of 100 W, while maintaining the temperature at 70°C for 2 and 4 hours. Ultrasonic cavitation improves mass transfer and enhances the formation of crystalline structures in a shorter time frame compared to hydrothermal treatment.

Following the synthesis, the resultant products were filtered to remove residual reagents and washed with distilled water until the filtrate reached a stable pH of 9– 10. The samples were subsequently dried at 100°C for 12 hours to obtain solid zeolite products suitable for characterization. To confirm the phase purity, structural properties, and morphology of the synthesized NaX zeolite, a suite of advanced analytical techniques was employed, including XRD for phase identification, FTIR for chemical bonding analysis, and SEM for morphological evaluation. This detailed synthesis protocol underscores the importance of controlled experimental conditions in achieving high-purity NaX zeolite and provides a foundation for comparative analysis between the hydrothermal and sonication methodologies.

2.5. Characterization of Synthesized NaX Zeolite

2.5.1. X-ray Diffraction (XRD)

XRD was employed to identify the crystalline phases and evaluate the phase purity of NaX zeolite. Measurements were performed using a Philips XRG 3100 diffractometer equipped with Cu-Kα radiation, scanned over a 2θ range of 5° to 60°. Both hydrothermal and sonication products were analyzed to detect phase transitions and crystallinity differences.

2.5.2. Fourier-Transform Infrared Spectroscopy (FTIR)

FTIR spectra were recorded using a Perkin Elmer Spectrum GX spectrometer to investigate the chemical bonding and functional groups of the zeolite framework. Characteristic absorption bands such as O–H stretching (3500–3200 cm^{-1}), H–O–H bending (~1650 cm^{-1}), and T– O–T stretching vibrations (1250–950 cm^{-1}) were examined to confirm the formation of NaX zeolite.

2.5.3. Scanning Electron Microscopy (SEM)

SEM analysis was carried out using a Hitachi S-570 instrument operated at 15 kV. The morphology, crystal shape, and size distribution of the synthesized NaX zeolite were observed for both synthesis methods to evaluate the degree of crystal formation and structural uniformity.

3. Results and Discussion

3.1. Pre-treatment: Alkali Fusion

Characteristic of Blitar kaolin based on XRF analysis reported in our previous study [16], Blitar kaolin primarily consists of silica (Si) and alumina (Al). Following HCl washing, the Si content increased from 65.4% to 75.2%, while the Al content decreased from 12% to 8.8%. This shift in the Si/Al ratio indicates a substantial removal of impurities and an enrichment of silica, enhancing the suitability of the kaolin as a high-silica precursor for NaX zeolite synthesis.

The XRD analysis (Figure 1) reveals that kaolin contains substantial quartz impurities, which pose a challenge to its direct use in zeolite synthesis. The alkali fusion process effectively reduces the intensity of both kaolin and quartz peaks, as evidenced by the XRD patterns, with increasing amounts of NaOH facilitating this transformation. At a NaOH/kaolin weight ratio of 1.0, the reduction in quartz intensity is accompanied by the emergence of distinct peaks corresponding to Na_2SiO_3, indicating partial conversion.

The process achieves complete transformation with higher ratios of 2.0 and 3.0, producing pure Na_2SiO_3. This suggests that quartz dissolves into Na_2SiO_3 under the synergistic effects of thermal and alkali activation. The

maximum intensity of Na_2SiO_3 peaks observed at a NaOH/kaolin weight ratio of 3.0 indicates optimal conditions for its formation. These findings underline the critical role of the alkali fusion process in enhancing the reactivity of kaolin by minimizing quartz content and generating a suitable precursor for zeolite synthesis.

The alkali fusion treatment significantly alters the crystallinity of raw kaolin, as evidenced by reduced intensity and eventual disappearance of quartz and kaolinite peaks in the XRD patterns (Figure 1). This reduction in crystallinity is attributed to the disruption of the layered aluminosilicate structure, resulting in the formation of an amorphous Na_2SiO_3 phase. The decrease in structural order facilitates the depolymerization of silicate and aluminate frameworks, thereby enhancing the chemical reactivity of the precursor. This amorphous state is beneficial for zeolite synthesis, as it supports the rearrangement and nucleation of framework species into more ordered, crystalline structures. These findings align with previous reports indicating that alkali-induced decrystallization is a critical step in producing high-purity, highly crystalline faujasite-type zeolites [18].

The FTIR spectrum (Figure 2) provides critical insights into the compositional and structural changes in kaolin during the alkali fusion process. The initial kaolin spectrum reveals prominent silica vibrations at 754 cm^{-1}, indicating substantial quartz impurities. In addition, the spectrum exhibits several well-defined absorption bands indicative of kaolin's layered aluminosilicate structure. These include Al-OH stretching vibrations at 3699 and 3450 cm^{-1}, associated with the hydroxyl groups in the octahedral layer, and water bending vibrations at 1633 cm^{-1}, attributable to interlayer water molecules. The tetrahedral asymmetric T-O-T (T = Si or Al) stretching mode at 1037 cm^{-1} further confirms the presence of silica-alumina frameworks, while the octahedral Al-OH stretching band at 912 cm^{-1} reflects the aluminum coordination environment. The symmetric T-O-T bending vibrations appear at 694 and 528 cm^{-1}, with asymmetric bending observed at 493 cm^{-1}, collectively representing the structural integrity of the kaolin matrix.

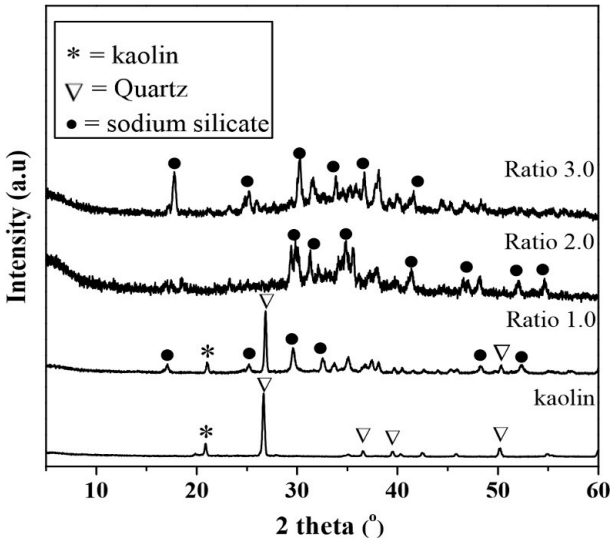

Figure 1. The XRD patterns of kaolin and alkali fusion products

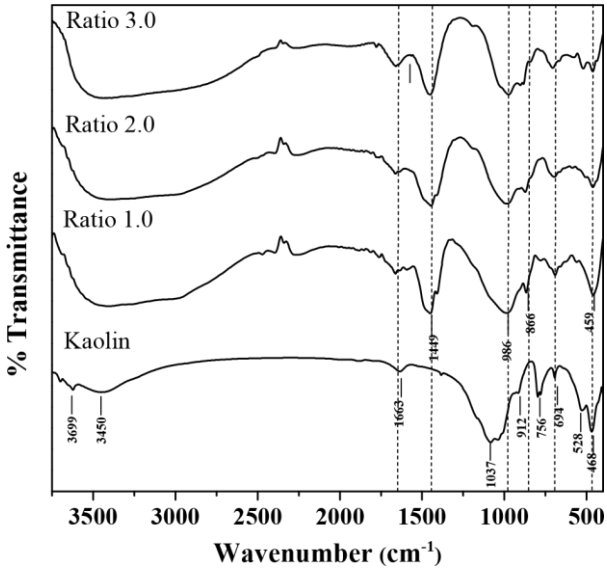

Figure 2. The FTIR spectra of kaolin and alkali fusion products

Upon alkali fusion, the kaolin undergoes a marked transformation, as evidenced by the emergence of distinct absorption bands at 986, 984, and 974 cm^{-1}. These bands are characteristic of tetrahedral asymmetric T-O-T stretching vibrations in the Na_2SiO_3 structure, signifying the conversion of kaolin into a reactive Na_2SiO_3 phase. This transformation is driven by the dissolution of quartz and the disruption of the original silica-alumina network under the combined effects of thermal and alkali activation.

The observed spectral changes confirm the successful reduction of quartz impurities and highlight the formation of a more amorphous and reactive precursor, which is essential for subsequent zeolite synthesis. This detailed analysis underscores the utility of FTIR spectroscopy in elucidating the molecular-level changes that occur during the alkali fusion process, providing a robust framework for optimizing precursor preparation in advanced material synthesis.

The morphological evolution of kaolin during the alkali fusion process was comprehensively analyzed using SEM, as depicted in Figure 3. The SEM images of natural kaolin reveal a distinctive layered structure characterized by the stacking of tetrahedral silica and octahedral alumina sheets. This well-ordered arrangement is typical of kaolin minerals, where the interlayer interactions are stabilized by hydrogen bonding. Such a structure contributes to the material's inherent chemical inertness and limited reactivity in its raw state.

Upon alkali fusion with a NaOH/kaolin weight ratio of 1.0, the SEM micrographs indicate that the Na_2SiO_3 retains a partially layered morphology. This observation suggests that the thermal and chemical disruption of the alumina and silica stacking is incomplete, with residual structural elements from the original kaolin framework still apparent. The limited transformation at this stage highlights the insufficient dissolution of quartz and the partial conversion of kaolin into a more reactive form.

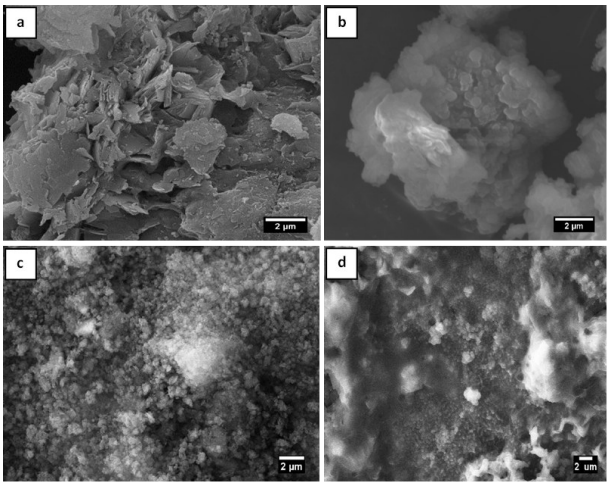

Figure 3. Micrographs of (a) kaolin and alkali fusion products prepared at NaOH/kaolin weight ratios of (b) 1.0, (c) 2.0, and (d) 3.0

As the NaOH/kaolin weight ratio increases to 2.0, the morphology undergoes a significant transformation, exhibiting irregular structures with no discernible layering. This change reflects the complete dissolution of the original kaolin framework and the reorganization of the material into an amorphous Na_2SiO_3 phase. The irregularity and heterogeneity in morphology at this stage can be attributed to the synergistic effects of thermal energy and alkali activation, which facilitate the breakdown of both tetrahedral and octahedral layers into a more disordered but highly reactive state.

At a weight ratio of 3.0, the morphology becomes increasingly irregular and assumes a cloud-like appearance. This drastic morphological shift is associated with the hygroscopic properties of Na_2SiO_3, which readily absorbs moisture from the environment, leading to structural expansion and deformation. The SEM images at this stage reveal a material with high porosity and surface area, which are advantageous for subsequent zeolite synthesis. These findings highlight the critical role of NaOH concentration in dictating the degree of structural disintegration and morphological evolution, underscoring the importance of optimizing alkali fusion parameters for efficient precursor preparation.

This detailed morphological assessment not only elucidates the structural transitions occurring during the alkali fusion process but also provides valuable insights into the physicochemical mechanisms underlying the conversion of natural kaolin into Na_2SiO_3. Such understanding is pivotal for advancing the synthesis of high-purity zeolites and other functional materials.

3.2. Sonication and Hydrothermal Method for Zeolite Synthesis

The alkali fusion product prepared with a NaOH/kaolin weight ratio of 2.0 was employed as a precursor to evaluate the efficacy of sonication and hydrothermal methods for NaX zeolite synthesis. The XRD patterns of the synthesized NaX zeolite exhibit prominent diffraction peaks at 2θ = 6.05°, 9.49°, 22.28°, and 26.67°, which correspond well with the standard reference values for NaX zeolite listed in the Joint Committee on Powder Diffraction Standards (JCPDS 39-0238). These peaks confirm the formation of a phase-pure NaX structure in the 2-hour crystallization samples.

The diffractogram results of the hydrothermal method, presented in Figure 4, reveal that a crystallization time of 2 hours produces pure NaX zeolite. This is confirmed by the presence of characteristic diffraction peaks at 2θ values of 6.05° and 26.67°, which correspond to the standard crystallographic reflections of NaX zeolite. However, when the crystallization duration is extended to 4 hours, the diffractogram indicates the formation of sodalite impurities, evidenced by additional peaks at 2θ values of 14.5° and 24.9°, which align with the standard pattern for sodalite.

The appearance of characteristic NaX diffraction peaks at 2θ values of 6.05° and 26.67° after 2 hours of hydrothermal crystallization aligns with the findings of Samadhi *et al.* [13], who reported similar peak positions for NaX synthesized from kaolin using alkali fusion. Additionally, the formation of sodalite as a secondary phase at 4 hours is consistent with the report by Foroughi *et al.* [14], which showed that prolonged crystallization favors thermodynamically stable phases such as sodalite.

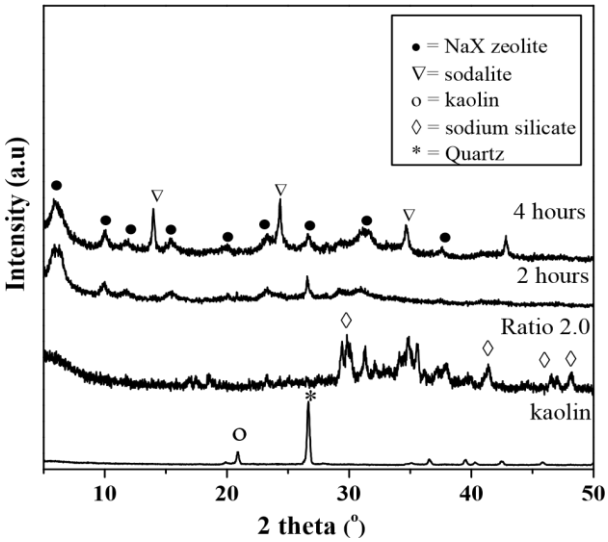

Figure 4. The XRD patterns of hydrothermal products

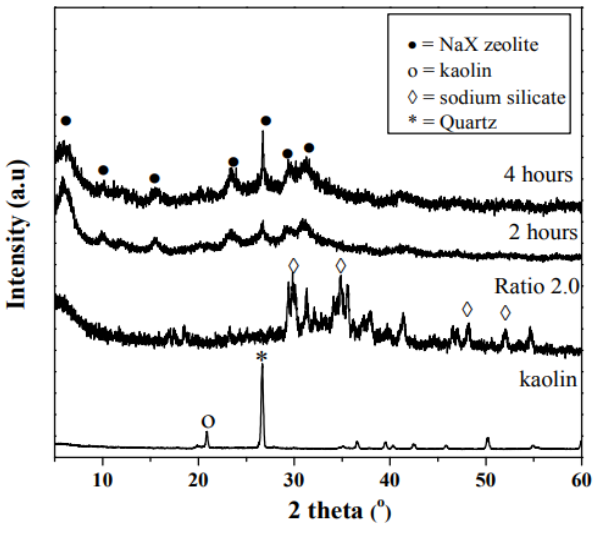

Figure 5. The XRD patterns of sonication products

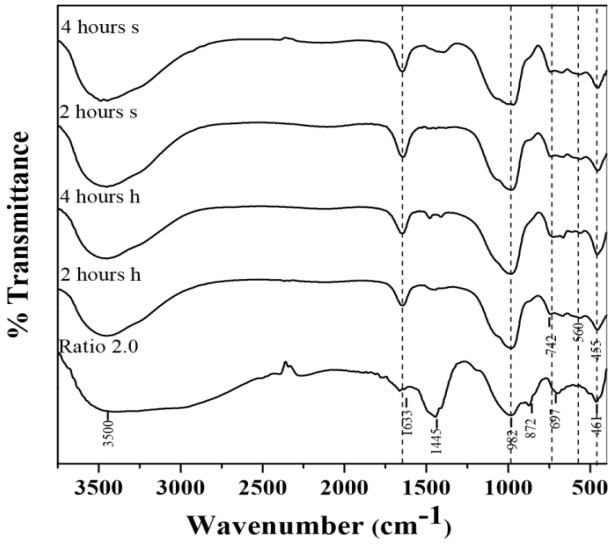

Figure 6. The FTIR spectra of synthesized products (s = sonication, h = hydrothermal)

These findings underscore the critical influence of crystallization time on the phase purity and composition of the synthesized product. The transition from NaX zeolite to sodalite with prolonged crystallization time aligns with Ostwald's rule of stages, which suggests that metastable phases such as NaX and NaA zeolites may dissolve over time, giving way to the formation of thermodynamically more stable phases like sodalite. This phenomenon reflects a dynamic equilibrium during the crystallization process, where increased reaction times provide sufficient energy and mobility to rearrange silicate and aluminate species into a more stable sodalite framework.

The XRD analysis of the samples synthesized using the sonication method (Figure 5) demonstrates the successful formation of pure NaX zeolite at both 2-hour and 4-hour crystallization durations. The characteristic diffraction peaks corresponding to NaX zeolite are present in both samples, confirming phase purity. However, the sample subjected to a 4-hour crystallization process exhibits sharper and more intense diffraction peaks, indicative of higher crystallinity. This observation highlights that extended crystallization time under ultrasonic conditions promotes a more ordered and well-defined zeolite framework.

The enhanced crystallinity observed in the 4-hour sample underscores the role of sonication in facilitating the crystallization process. The ultrasonic energy, delivered at a frequency of 42 kHz and power of 100 W, provides continuous agitation and cavitation effects, which enhance the diffusion of reactant species and promote nucleation and crystal growth. These dynamic conditions reduce the likelihood of defect formation and contribute to developing a highly crystalline zeolite structure.

Moreover, the ability of the sonication method to consistently produce high-purity NaX zeolite across different crystallization times highlights its robustness and efficiency compared to traditional hydrothermal methods. While the hydrothermal method is limited by time-dependent phase transformations, the sonication process maintains phase stability over prolonged durations, emphasizing its potential as a superior alternative for zeolite synthesis.

Our findings are consistent with those of Ojumu *et al.* [20], who reported that sonication accelerates zeolite formation and improves product purity compared to hydrothermal synthesis. Jusoh *et al.* [23] further confirmed that sonication enhances nucleation and reduces impurity formation in NaX. Similarly, Khaleque *et al.* [24] demonstrated that sonication leads to more uniform and stable NaX zeolite structures, even under varying crystallization times. These studies support the conclusion that ultrasonic methods offer a superior approach to zeolite synthesis, particularly in maintaining phase purity and reducing synthesis time.

The FTIR spectra shown in Figure 6 provide clear evidence of the transformation of Na_2SiO_3 into NaX zeolite, as indicated by the appearance of distinct absorption bands. Broad O–H stretching vibrations between 3500–3200 cm^{-1} suggest the presence of surface hydroxyl groups and adsorbed water, typical of zeolitic materials. This is further supported by the O-H bending vibrations at 1650–1600 cm^{-1}, reflecting the interaction of water within the zeolite framework. Additionally, the asymmetric T-O-T (tetrahedral Si-O-Si or Si-O-Al) stretching vibrations in the 1250–950 cm^{-1} range indicate the successful incorporation of silicate and aluminate units, characteristic of the NaX zeolite structure. External asymmetric T-O-T stretching bands between 1150 and 1050 cm^{-1} further confirm the formation of a robust tetrahedral framework within the zeolite.

Moreover, the internal symmetric T–O–T stretching vibrations between 720–650 cm^{-1} and external symmetric bands between 820–720 cm^{-1} confirm the stability of the NaX zeolite framework. A key feature of NaX is the presence of D6R (double six-ring) vibrations in the 650–500 cm^{-1} range, which correspond to the faujasite structural units—key indicators of successful crystallization. The emergence of these characteristic bands, which are intrinsically linked to the D6R structure, confirms the successful crystallization of NaX zeolite. The asymmetric T-O-T stretching vibrations observed in the 1250–950 cm^{-1} region correspond to the framework vibrations of Si–O–Si and Si–O–Al bonds, as previously described by Krachuamram *et al.* [4], further confirming the successful formation of NaX zeolite structure.

Figure 7 depicts the morphological evolution of NaX zeolite synthesized by hydrothermal and sonication methods at different crystallization times, based on SEM analysis. After 2 hours of crystallization using the hydrothermal method, the resulting particles exhibit an irregular and disordered morphology, suggesting incomplete crystal formation at this stage. However, extending the crystallization time to 4 hours promotes the development of more well-defined, cubic-shaped crystals, characteristic of the NaX zeolite structure. This shift indicates that prolonged hydrothermal treatment enhances nucleation and crystal growth, leading to more uniform and stable zeolite particles.

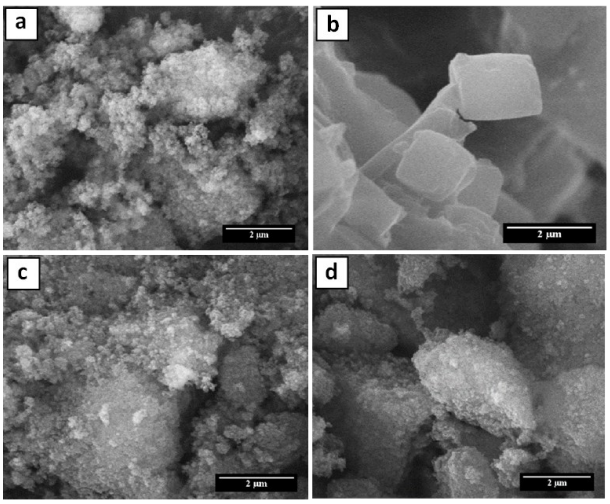

Figure 7. Micrographs of synthesized products obtained by (a) hydrothermal method at 2 hours, (b) hydrothermal method at 4 hours, (c) sonication method at 2 hours, and (d) sonication method at 4 hours

In comparison, the sonication method also produces irregular-shaped particles after 2 hours of crystallization, similar to the hydrothermal process at the same duration. However, after 4 hours of ultrasonic treatment, the morphology transitions to more well-formed crystalline shapes, with notable improvements in structural regularity and definition. The high-energy sonication environment likely accelerates nucleation by providing continuous agitation and cavitation effects, promoting rapid crystallization. This suggests that while both methods can achieve well-crystallized NaX zeolite, the sonication process is more efficient at driving uniform crystal growth in shorter timeframes.

The comparative analysis of the SEM images reveals that the hydrothermal method, particularly at extended crystallization times, produces finer particles with more uniform dimensions compared to the sonication method. This observation may be attributed to the controlled heat and pressure environment in hydrothermal synthesis, which offers greater regulation over the crystal growth process. In contrast, the sonication method, though faster in promoting crystallization, may induce higher particle heterogeneity due to the dynamic nature of ultrasonic energy.

After 4 hours of hydrothermal treatment, the appearance of well-defined cubic crystals is in agreement with the study by García-Villén *et al.* [21], which showed improved morphology with extended crystallization. Conversely, SEM images from the sonication method after 2 hours revealed more irregular and heterogeneous particles, similar to the results observed by Jusoh *et al.* [23], who noted that ultrasonic irradiation often leads to rapid but less uniform crystal growth.

In summary, these findings suggest that while the sonication method excels in accelerating crystallization and producing well-defined NaX crystals in a shorter time, the hydrothermal approach offers superior control over particle size and uniformity, particularly with extended crystallization periods. The choice between these methods should, therefore, be guided by the desired balance between crystallization speed, particle morphology, and application-specific performance characteristics of the synthesized zeolite.

These findings are consistent with previous research showing the distinct advantages of both methods. Khaleque *et al.* [24] reported that sonication improves crystallization speed and yields higher-purity NaX zeolite with fewer secondary phases compared to hydrothermal synthesis. Jusoh *et al.* [23] further demonstrated that sonication enhances nucleation kinetics and prevents sodalite formation even at longer durations. Moreover, Askari *et al.* [25] confirmed that sonication improves phase stability and crystallinity, making it a promising method for efficient, scalable NaX zeolite production. These studies support the conclusion that sonication is highly effective for producing high-quality NaX zeolite in a shorter time, while hydrothermal synthesis remains valuable for controlling particle size and uniformity.

4. Conclusion

NaX zeolite was successfully synthesized from Blitar kaolin through alkali fusion pre-treatment, followed by hydrothermal and sonication methods. The sonication method demonstrated superior performance, producing high-purity NaX zeolite with well-defined cubic morphology and enhanced crystallinity in shorter crystallization times compared to the hydrothermal method, which exhibited sodalite impurities at extended durations. Among the tested parameters, a NaOH/kaolin weight ratio of 2.0 was found to be optimal for producing a reactive Na_2SiO_3 precursor, which ultimately enhanced the phase purity and crystallinity of the resulting NaX zeolite. SEM and XRD analyses confirmed the structural integrity of the synthesized zeolite, while FTIR spectroscopy verified the characteristic NaX framework. The findings highlight the potential of sonication as a time-efficient and scalable approach for synthesizing high-purity NaX zeolite, offering significant advantages for industrial applications in catalysis, adsorption, and ion exchange. The choice between the sonication and hydrothermal methods should be carefully considered based on the desired balance between crystallization speed, particle morphology, and the specific performance characteristics required for the intended application. As demonstrated in our study, the sonication method excels in accelerating crystallization and producing high-purity NaX zeolite in a shorter time, making it highly suitable for industrial-scale production and time-sensitive applications. In contrast, the hydrothermal method allows for better control over particle size and uniformity, especially during extended crystallization, which may be advantageous for applications requiring precise morphological control.

References

[1] Arthur Abinader Vasconcelos, Thomas Len, Alex de Nazaré de Oliveira, Ana Alice Farias da Costa, Allan Rodrigo da Silva Souza, Carlos Emmerson Ferreira da Costa, Rafael Luque, Geraldo Narciso da Rocha Filho, Renata Coelho Rodrigues Noronha, Luís Adriano Santos do Nascimento, Zeolites: A Theoretical and Practical Approach with Uses in

(Bio)Chemical Processes, *Applied Sciences*, 13, 3, (2023), 1897 https://doi.org/10.3390/app13031897

[2] Susi Nurul Khalifah, Udi Tyas, Saidun Fiddaroini, Suci Amalia, Pengaruh Pemeraman dan Suhu Pada Sintesis Zeolit Y dari Lumpur, *ALCHEMY: Journal of Chemistry*, 10, 1, (2022), 27-32 https://doi.org/10.18860/al.v10i1.17334

[3] Álvaro de Jesús Ruíz-Baltazar, Advancements in nanoparticle-modified zeolites for sustainable water treatment: An interdisciplinary review, *Science of The Total Environment*, 946, (2024), 174373 https://doi.org/10.1016/j.scitotenv.2024.174373

[4] Somkiat Krachuamram, Kingkaew Chayakul Chanapattharapol, Nuntaporn Kamonsutthipaijit, Synthesis and characterization of NaX-type zeolites prepared by different silica and alumina sources and their CO_2 adsorption properties, *Microporous and Mesoporous Materials*, 310, (2021), 110632 https://doi.org/10.1016/j.micromeso.2020.110632

[5] Wen Xiao, Peng Dong, Chan Wang, Jingdong Xu, Tiesen Li, Haibo Zhu, Tinghai Wang, Renwei Xu, Yuanyuan Yue, Facile synthesis of hierarchical NaX zeolite from natural kaolinite for efficient Knoevenagel condensation, *Chinese Journal of Chemical Engineering*, 65, (2024), 75-84 https://doi.org/10.1016/j.cjche.2023.07.007

[6] Valentina Verdoliva, Michele Saviano, Stefania De Luca, Zeolites as Acid/Basic Solid Catalysts: Recent Synthetic Developments, *Catalysts*, 9, 3, (2019), 248 https://doi.org/10.3390/catal9030248

[7] Yasemin Erten-Kaya, Fehime Cakicioglu-Ozkan, Effect of ultrasound on the kinetics of cation exchange in NaX zeolite, *Ultrasonics Sonochemistry*, 19, 3, (2012), 701-706 https://doi.org/10.1016/j.ultsonch.2011.10.010

[8] Hanaa Merad-Dib, Chahrazed Bendenia, Souhila Bendenia, Adsorption of an organic pollutant in to exchanged NaX zeolite: Thermodynamic study, *Desalination and Water Treatment*, 320, (2024), 100789 https://doi.org/10.1016/j.dwt.2024.100789

[9] Jiaxing Guo, Hong Wu, Yao Wei, Yingju Miao, Jingyuan Qu, Ping Wang, Synthesis of a high-iron fly-ash-based Na-X molecular sieve and its application in the adsorption of low concentration of CO_2, *RSC Advances*, 14, 3, (2024), 1686-1696 https://doi.org/10.1039/D3RA07615F

[10] Priyanka Roy, Nandini Das, Synthesis of NaX zeolite-graphite amine fiber composite membrane: Role of graphite amine in membrane formation for H_2/CO_2 separation, *Applied Surface Science*, 480, (2019), 934-944 https://doi.org/10.1016/j.apsusc.2019.03.038

[11] Vita Nur Iftitahiyah, Didik Prasetyoko, Hadi Nur, Hasliza Bahruji, Hartati Hartati, Synthesis and characterization of zeolite NaX from Bangka Belitung Kaolin as alternative precursor, *Malaysian Journal of Fundamental and Applied Sciences*, 14, 4, (2018), 414-418 https://doi.org/10.11113/mjfas.v14n4.964

[12] Altantuya Ochirkhuyag, Jadambaa Temuujin, The Catalytic Potential of Modified Clays: A Review, *Minerals*, 14, 6, (2024), 629 https://doi.org/10.3390/min14060629

[13] Tjokorde Walmiki Samadhi, Subagjo Subagjo, Kevin R. Lismana, Khasin Fuadi, Synthesis of γ -Al_2O_3 Catalyst Support from Kaolin of Indonesian Origin, *Journal of Engineering and Technological Sciences*, 43, 2, (2013), 113-126 https://doi.org/10.5614/itbj.eng.sci.2011.43.2.3

[14] Mahsa Foroughi, Amin Salem, Shiva Salem, Characterization of phase transformation from low grade kaolin to zeolite LTA in fusion technique: Focus on quartz melting and crystallization in presence of $NaAlO_2$, *Materials Chemistry and Physics*, 258, (2021), 123892 https://doi.org/10.1016/j.matchemphys.2020.123892

[15] Hartati, Didik Prasetyoko, Mardi Santoso, Imroatul Qoniah, Wai L. Leaw, Putri B. D. Firda, Hadi Nur, A review on synthesis of kaolin-based zeolite and the effect of impurities, *Journal of the Chinese Chemical Society*, 67, 6, (2020), 911-936 https://doi.org/10.1002/jccs.201900047

[16] S. N. Khalifah, Z. N. aini, E. K. Hayati, N. Aini, A. Prasetyo, Synthesis and characterization of mesoporous NaY zeolite from natural Blitar's kaolin, *IOP Conference Series: Materials Science and Engineering*, 333, 1, (2018), 012005 https://doi.org/10.1088/1757-899X/333/1/012005

[17] John Vogrin, Talitha Santini, Hong Peng, Ling Zhao, James Vaughan, Synthesis of zeolites using kaolin in concentrated sodium hydroxide-aluminate solutions, *Applied Clay Science*, 244, (2023), 107106 https://doi.org/10.1016/j.clay.2023.107106

[18] Stephen Otieno, Chrispin Kowenje, Fredrick Kengara, Robert Mokaya, Effect of kaolin pre-treatment method and NaOH levels on the structure and properties of kaolin-derived faujasite zeolites, *Materials Advances*, 2, 18, (2021), 5997-6010 https://doi.org/10.1039/D1MA00449B

[19] Colin S. Cundy, Paul A. Cox, The Hydrothermal Synthesis of Zeolites: History and Development from the Earliest Days to the Present Time, *Chemical Reviews*, 103, 3, (2003), 663-702 https://doi.org/10.1021/cr020060i

[20] Tunde V. Ojumu, Pieter W. Du Plessis, Leslie F. Petrik, Synthesis of zeolite A from coal fly ash using ultrasonic treatment – A replacement for fusion step, *Ultrasonics Sonochemistry*, 31, (2016), 342-349 https://doi.org/10.1016/j.ultsonch.2016.01.016

[21] Fátima García-Villén, Eduardo Flores-Ruíz, Cristóbal Verdugo-Escamilla, F. Javier Huertas, Hydrothermal synthesis of zeolites using sanitary ware waste as a raw material, *Applied Clay Science*, 160, (2018), 238-248 https://doi.org/10.1016/j.clay.2018.02.004

[22] Lucija Majal Belca, Aleš Ručigaj, Dušan Teslič, Matjaž Krajnc, The use of ultrasound in the crystallization process of an active pharmaceutical ingredient, *Ultrasonics Sonochemistry*, 58, (2019), 104642 https://doi.org/10.1016/j.ultsonch.2019.104642

[23] Norwahyu Jusoh, Yin Fong Yeong, Maisarah Mohamad, Kok Keong Lau, Azmi M. Shariff, Rapid-synthesis of zeolite T via sonochemical-assisted hydrothermal growth method, *Ultrasonics Sonochemistry*, 34, (2017), 273-280 https://doi.org/10.1016/j.ultsonch.2016.05.033

[24] Abdul Khaleque, Md Masruck Alam, Mozammel Hoque, Shuvodip Mondal, Jahid Bin Haider, Bentuo Xu, M. A. H. Johir, Aneek Krishna Karmakar, J. L. Zhou, Mohammad Boshir Ahmed, Mohammad Ali Moni, Zeolite synthesis from low-cost materials and environmental applications: A review, *Environmental Advances*, 2, (2020), 100019 https://doi.org/10.1016/j.envadv.2020.100019

[25] Sima Askari, Shayan Miar Alipour, Rouein Halladj, Mohammad Hossein Davood Abadi Farahani, Effects of ultrasound on the synthesis of zeolites: a review, *Journal of Porous Materials*, 20, 1, (2013), 285-302 https://doi.org/10.1007/s10934-012-9598-6